

# Submillisecond response variable optical attenuator based on sheared polymer network liquid crystal

Yung-Hsun Wu, Yi-Hsin Lin, Yan-Qing Lu, Hongwen Ren, Yun-Hsing Fan, Janet R. Wu, and Shin-Tson Wu

College of Optics and Photonics, University of Central Florida, Orlando, Florida 32816  
[swu@mail.ucf.edu](mailto:swu@mail.ucf.edu)

<http://lcd.creol.ucf.edu>

**Abstract:** We demonstrate a variable optical attenuator (VOA) at  $\lambda=1.55\ \mu\text{m}$  using a sheared polymer network liquid crystal (SPNLC). The SPNLC exhibits a fast response time and weak wavelength dependency. Comparing with other polymer-stabilized liquid crystals, the SPNLC has lower driving voltage and negligible light scattering loss when the wavelength exceeds 700 nm. A reflection type VOA with  $\sim 0.24$  ms response time and  $-32$  dB dynamic range is demonstrated at room temperature and 35 V<sub>rms</sub> voltage.

©2004 Optical Society of America

**OCIS codes:** (230.3720) Liquid-crystal devices; (160.5470) Polymers

---

## References and links

1. R. A. Soref and D. H. McMahon, "Total switching of unpolarized fiber light with a four-port electro-optic liquid-crystal device," *Opt. Lett.* **5**, 147-149 (1980).
2. E. G. Hanson, "Polarization-independent liquid-crystal optical attenuator for fiber optics applications," *Appl. Opt.* **21**, 1342-1344 (1982).
3. K. Hirabayashi, M. Wada, and C. Amano, "Optical-fiber variable-attenuator arrays using polymer-network liquid crystal," *IEEE Photon. Technol. Lett.* **13**, 487-489 (2001).
4. J. J. Pan, H. Wu, W. Wang, X. Qiu, and J. Jiang, "Temperature independent, accurate LC VOA through electric feedback control," in *Proceedings of National Fiber Optics Engineers Conference (Telcordia, Orlando, Florida, 2003)*, 943-949.
5. C. Mao, M. Xu, W. Feng, T. Huang, K. Wu, and J. Wu, "Liquid-crystal applications in optical telecommunication," in *Liquid Crystal Materials, Devices, and Applications IX*, L. C. Chien, ed., Proc. SPIE **5003**, 121-129 (2003).
6. S. T. Wu and D. K. Yang, *Reflective Liquid Crystal Displays* (Wiley, New York, 2001).
7. S. Gauza, H. Wang, C. H. Wen, S. T. Wu, A. J. Seed and R. Dąbrowski, "High birefringence isothiocyanato tolane liquid crystals," *Jpn. J. Appl. Phys. Part 1* **42**, 3463-3466 (2003).
8. R. A. M. Hikmet, "Electrically induced light scattering from anisotropic gels," *J. Appl. Phys.* **68**, 4406-4412 (1990).
9. Y. Q. Lu, F. Du, Y. H. Lin and S. T. Wu, "Variable optical attenuator based on polymer-stabilized twisted nematic liquid crystal," *Opt. Express* **12**, 1221-1227 (2004).  
<http://www.opticsexpress.org/abstract.cfm?URI=OPEX-12-7-1221>
10. F. Du, Y. Q. Lu, H. W. Ren, S. Gauza, and S. T. Wu, "Polymer-stabilized cholesteric liquid crystal for polarization-independent variable optical attenuator," *Jpn. J. Appl. Phys.* **43**, 7083-7086 (2004).
11. F. Du, S. Gauza, and S. T. Wu, "Influence of curing temperature and high birefringence on the properties of polymer-stabilized liquid crystals," *Opt. Express* **11**, 2891-2896 (2003).  
<http://www.opticsexpress.org/abstract.cfm?URI=OPEX-11-22-2891>
12. J. L. West, G. Zhang, and A. Glushchenko, "Stressed liquid crystals for electrically controlled fast shift of phase retardation," *Soc. Information Display, Tech. Digest* **34**, 1469-1471 (2003).
13. Y. H. Fan, Y. H. Lin, H. Ren, S. Gauza, and S. T. Wu, "Fast-response and scattering-free polymer network liquid crystals for infrared light modulators," *Appl. Phys. Lett.* **84**, 1233-1235 (2004).
14. O. A. Aphonin, Y. V. Panina, A. B. Pravdin, and D. A. Yakovlev, "Optical-properties of stretched polymer-dispersed liquid-crystal films," *Liq. Cryst.* **15**, 395-407 (1993).
15. I. Amimori, J. N. Eakin, G. P. Crawford, N. V. Priezjev, and R. A. Pelcovits, "Optical and mechanical properties of stretched PDLC films for scattering polarizers," *Soc. Information Display, Tech. Digest* **33**, 834-837 (2002).

16. P. Sixou, C. Gautier, and H. Villanova, "Nematic and cholesteric PDLC elaborated under shear stress," *Mol. Cryst. Liq. Cryst.* **364**, 679-690 (2001).
  17. V. Vorflusev and S. Kumar, "Phase-separated composite films for liquid crystal displays" *Science* **283**, 1903-1905 (1999).
- 

## 1. Introduction

Nematic liquid crystal (LC)-based variable optical attenuator (VOA) has been used widely for fiber-optic telecommunications because of its low cost, gray scale capability, low optical loss, and low power consumption [1-5]. For these applications, fast response time (<1 ms) and large dynamic range (>30 dB) are highly desirable. The response time of a LC device is mainly determined by the visco-elastic coefficient ( $\gamma_1 / K_{11}$ ), LC cell gap ( $d$ ), and applied voltage [6]. In the near infrared ( $\lambda=1.55 \mu\text{m}$ ) region, to achieve  $1\pi$  phase retardation using a homogeneous cell the required  $d\Delta n$  (where  $\Delta n$  is the LC birefringence) is  $\lambda/2$ , or  $0.78 \mu\text{m}$ . High birefringence LC materials [7] help to reduce the required cell gap and therefore reduce the response time. However, high birefringence liquid crystals are usually associated with an increased viscosity and high melting temperature. The former can be overcome by operating VOA at an elevated temperature, but the latter is unfavorable for formulating eutectic mixtures. For practical applications, the melting temperature should be lower than  $-40^\circ\text{C}$  for the purpose of storage.

To obtain fast response time at room temperature, various polymer-stabilized liquid crystal (PSLC; also known as anisotropic gel) approaches have been investigated [8-11]. In a PSLC, the polymer concentration is 3-8 wt %. The response time decreases as the polymer concentration increases. Two problems associated with the LC gels are strong light scattering and high operating voltage. As the polymer concentration increases, the operating voltage increases substantially.

Recently, stressed liquid crystal [12] and polymer-network liquid crystal (PNLC) [13] have been developed for achieving fast response time and scattering-free phase modulators. In a PNLC, rod-like monomers are used and the substrate surfaces are treated with homogeneous alignment. Usually, a PNLC exhibits strong light scattering in the visible spectral region. To suppress light scattering at  $\lambda=1.55 \mu\text{m}$ , a minimal polymer concentration of  $\sim 10\%$  is required in order to make domain sizes smaller than the wavelength. Under such a circumstance, the LC domains are surrounded by polymer networks so that the required operating voltage is increased substantially ( $\sim 7 V_{\text{rms}} / \mu\text{m}$ ).

Mechanical shearing of LC layer has been investigated on the starching plasticized PVA films containing 5-20 wt % LC for making scattering-type polarizers [14,15]. Similar shearing technique has also been applied to the polymer-dispersed LC composites for improving response time and reducing light scattering [12, 16]. The major difference between stressed LC and PNLC is that the stressed LC uses a softer monomer NOA-65 ( $\sim 15$  wt %) and does not require surface alignment. A major technical challenge for the stressed LC is that it requires mechanical shearing after the two-step UV curing in order to eliminate light scattering. Before shearing, the cell scatters light strongly. After shearing, the cell becomes highly transparent in the near IR region. The stressed LC has potential for display applications, provided that the operating voltage can be reduced and the light scattering in the blue region can be eliminated.

In this paper, we demonstrate a reflective-mode normally-on VOA using a sheared PNLC cell. The measured response time at room temperature is  $\sim 0.24$  ms and dynamic range is  $\sim 32$  dB at  $\lambda=1.55 \mu\text{m}$  and voltage  $V \sim 35 V_{\text{rms}}$ .

## 2. Sample fabrication

To prepare a PNLC cell, we mixed 15 wt % of photopolymerizable monomer (Norland optical adhesive NOA65) in a commercial Merck E7 LC mixture. The mixed LC and monomer was sandwiched between two ITO (indium-tin-oxide) glass substrates separated by two stripe

mylar spacers. The cell gap was controlled at  $\sim 9 \mu\text{m}$ . To polymerize the LC cell, a two-step UV curing process was adopted [12]. In the first step, the LC cell was illuminated to a UV light ( $\lambda \sim 365 \text{ nm}$ ,  $I = 50 \text{ mW/cm}^2$ ) for 15 min at  $T = 110 \text{ }^\circ\text{C}$ . The clearing temperature of E7 is  $\sim 60 \text{ }^\circ\text{C}$ . In the second step, the cell was cured in the same condition but at  $20 \text{ }^\circ\text{C}$ . Since the ITO glass has no surface treatment, the LC domains are randomly distributed so that the cell appears translucent after UV curing. In order to align the LC molecules in a uniform direction, we applied a shearing force to the top substrate while keeping the bottom glass substrate fixed. The shearing distance and speed were controlled by a precise motor motion system (Newport ESP-300). The shearing speed was controlled at  $0.1 \text{ mm/s}$  and the shearing distance was  $\sim 400 \mu\text{m}$ . After shearing, the PNLC cell became highly transparent. To prevent the sheared LC molecules from relaxing back, the peripherals of the cell were hermetically sealed by a UV adhesive. All our measurements were performed using the sealed LC cell. No noticeable performance change was detected before and after the hermetic sealing. Throughout this article, we abbreviate the sheared polymer-network liquid crystal as SPNLC.

Figure 1 shows the shearing processes and LC director orientation of a SPNLC cell. During UV exposure, the bottom substrate faced the UV light. After the two-step curing processes, a thin (sub-micron) isotropic polymer composite film [17] and polymer networks were formed. However, these LC microdomains in the polymer networks are randomly distributed, as sketched in Fig. 1(a). The film scatters light because of the refractive index mismatch between the LC and the polymer matrix. After shearing, the LC domains are aligned and light scattering is eliminated. Since the shearing force has gradient distribution, each layer of LC microdomains is expected to have different tilt angles, as depicted in Fig. 1(b). Near the top substrate, the shearing force is strong so that the LC domains are aligned nearly parallel to the substrate. Deeper from top substrate, the shearing torque is weaker so that the LC tilt angle is larger. This gradient tilt angle distribution makes important contributions to the electro-optic properties of the SPNLC cell. Firstly, the increased tilt angle smears the threshold behavior. For a PNLC without gradient tilt angle, its threshold voltage is quite high. Secondly, the gradient tilt angle lowers the dark state (between crossed polarizers) voltage. However, the gradient tilt angle reduces the effective birefringence of the LC layer. At  $\lambda = 1.55 \mu\text{m}$ , the effective birefringence of the E7/NOA65 mixture (85:15 wt % ratios) is  $\sim 0.17$ , but the average birefringence of the SPNLC is decreased to  $\sim 0.12$ . Some LC molecules could be imbedded in the polymer networks, but the major birefringence loss is believed to originate from the tilted LC alignment.

The response time of the SPNLC is governed by the domain size, shape, and polymer network binding strength, and is insensitive to the cell gap. We could increase the cell gap to obtain more phase change without sacrificing response time. The tradeoff is the increased voltage.

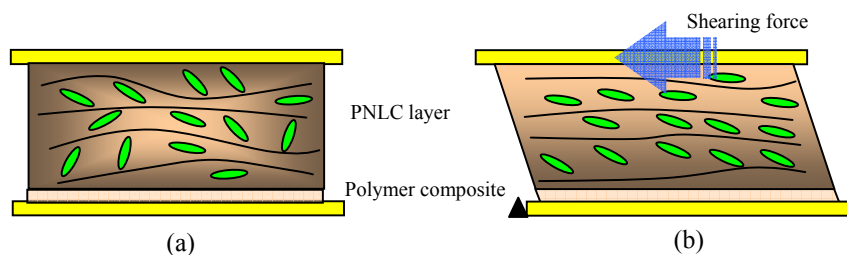


Fig. 1. Shearing processes and LC domain orientations of the SPNLC film. (a) Before and (b) after shearing.

### 3. Experiment and results

Figure 2 depicts the schematic diagram of a SPNLC-based VOA. The light source ( $\lambda = 1.55$

$\mu\text{m}$ ) could come from a tunable laser source (ANDO AQ4321D) or from an ASE light source. The port 1 of a fiber-optic circulator is connected to the light source, port 2 to the collimator with an 8-cm working distance from a mirror, and port 3 to an optical spectrometer or a photo-detector. A phase modulator module is located between the collimator and the dielectric mirror. An ac voltage is applied to the LC cell for controlling the phase retardation through LabVIEW data acquisition system. By adjusting the driving voltage, we can modulate the light transmittance of the phase modulator. The reflected light from the mirror through the phase modulator module is collected by the same collimator. The circulator redirects the reflected light to port 3 which is captured by a spectrometer or a detector.

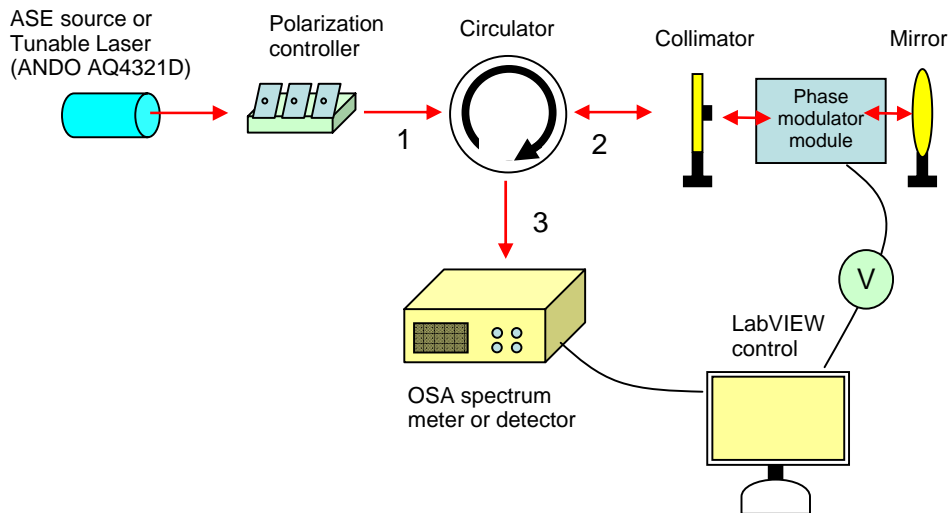


Fig. 2. The schematic diagram of a SPNLC-based VOA.

The detailed operation mechanism of the phase modulator module is illustrated in Figs. 3(a) and 3(b). The module contains a polarization beam displacer (PBD), a half-wave plate (HWP) which is laminated on the backside (upper half) of the PBD, a quarter-wave plate (QWP), and a SPNLC cell. Figure 3(a) shows the ON state (i.e.,  $V=0$ ) of the VOA. At  $V=0$ , the LC directors of the SPNLC cell are aligned along the sheared direction. The optical axes of the SPNLC and QWP are crossed, thus, their phase retardations are subtractive. Let us assume the incident light is unpolarized. When the light impinges the PBD, it is separated into two components: ordinary (top trace) and extraordinary (bottom) rays. The ordinary ray traverses through the HWP and becomes the extraordinary ray. At this stage, the incoming unpolarized light is converted to a linearly polarized light. In this experiment, the SPNLC cell is intentionally designed to possess a quarter-wave phase retardation ( $\delta=\pi/2$ ) at  $\lambda=1.55 \mu\text{m}$ . Thus, the phase of SPNLC cancels with that of QWP. Upon reflection from the mirror, the total phase difference of the outgoing beams from QWP remains 0. Therefore, two retro-beams have the same polarization states as they enter the QWP and will go back to the PBD along the same paths as shown in Fig. 3(a). This is the normally-on state of the VOA.

Figure 3(b) shows the off-state of the VOA. At  $V=35 V_{\text{rms}}$ , the phase retardation of the SPNLC cell is vanished (i.e.,  $\delta=0$  at  $\lambda=1.55 \mu\text{m}$ ). Therefore, the SPNLC cell causes no phase retardation to the incoming beams. The incoming beams only experience a  $\pi$  phase change after having passed the QWP twice. The polarization states of the top and bottom outgoing beams from QWP remain linear except that they have been rotated by  $90^\circ$ . As a result, they go back to the PBD at different paths. No light is coupled into the collimator, as shown in Fig. 3(b). This is the dark state of the VOA. The gray levels can be obtained by controlling the applied voltage.

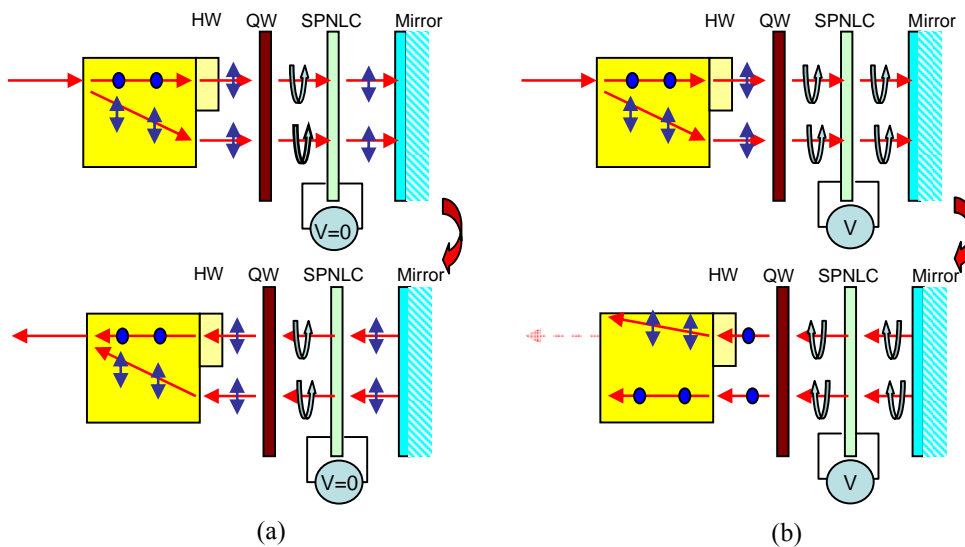


Fig. 3. The detailed operation mechanisms of the phase modulator module: (a) VOA ON state,  $V=0$ , and (b) VOA OFF state,  $V=35 V_{rms}$ . HW: half-wave plate, QW: quarter-wave plate, and SPNLC: sheared polymer network liquid crystal.

In experiment, we demonstrated a SPNLC-based VOA by using an Ando AQ4321D tunable laser operated at  $\lambda=1.55 \mu\text{m}$ . The output light is captured by a detector in port 3. We acquired the detector data by a LabVIEW computer program. Figure 4 plots the voltage-dependent VOA attenuation. The VOA was addressed by 10 kHz square waves. Little attenuation is observed below  $7.5 V_{rms}$ . This threshold voltage is  $\sim 3X$  lower than that of the PNLC cell using rod-like monomers and rubbed polyimide surface alignment layers [13]. The observed lower threshold voltage is believed to result from the gradient tilt angle of the LC domains, as illustrated in Fig. 1(b). As the applied voltage increases, the detected reflectance decreases almost linearly. At  $V=35 V_{rms}$ , the dynamic range reaches  $-32\text{dB}$ .

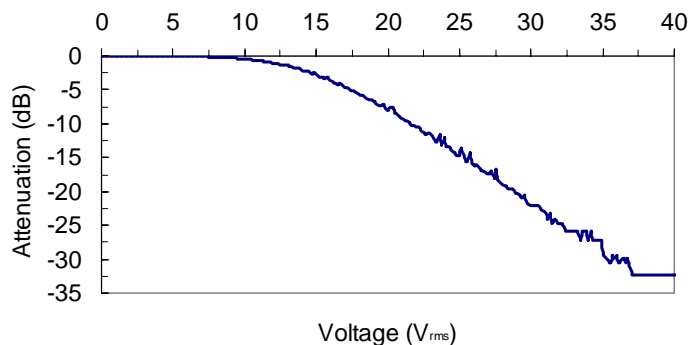


Fig. 4. The VOA attenuation at different drive voltages.  $\lambda=1.55 \mu\text{m}$ .

Figures 5(a) and 5(b) show the dynamic response of the SPNLC VOA. To measure the response time, a  $35 V_{rms}$  (upper traces) at  $f=10 \text{ kHz}$  square waves with 1 s duration was periodically applied to the VOA. The rise time and fall time are defined as 10 $\rightarrow$ 90% and

90→10% reflectance change, respectively. The measured optical response times are shown in the lower traces. Please note that this is a normally-on VOA. Figures 5(b) and 5(a) show the optical rise and decay times, respectively. From these figures, we find the rise time is 35  $\mu\text{s}$  and decay time 205  $\mu\text{s}$ . The faster turn-on time is due to the voltage effect and the slower decay time is due to the weaker elastic restoring force. Nevertheless, the response time of our SPNLC VOA is at least one order magnitude faster than the state-of-the-art nematic competitors. Such a fast response time is contributed by two physical mechanisms: sub-micron LC domain sizes and elliptical domain shapes. The latter is quite common for the polymer-dispersed LC droplets, especially with a shearing force. Based on the observed fast response time, we estimate that the LC domain size is around 0.5  $\mu\text{m}$ .

We also made SPNLC cells with different LC layer thicknesses. Results indicate that the response time is quite insensitive to the cell gap. This phenomenon is not surprising because the response time of a SPNLC is mainly determined by the LC domain size and shape. The cell gap does not play an important role here.

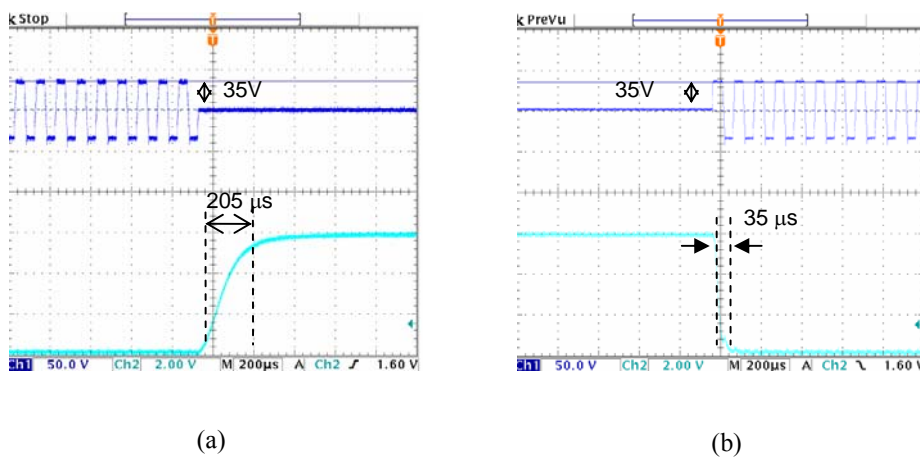


Fig. 5. Optical response time of the 9- $\mu\text{m}$  SPNLC VOA: (a) decay time, and (b) rise time.

We also measured the wavelength-dependent transmittance of the SPNLC cell. In order to calibrate for the surface reflections, a homogeneous LC cell filled with E7 was used as reference. Results are shown in Fig. 6. From Fig. 6, the SPNLC has ~15% scattering loss at  $\lambda \sim 500$  nm. As the wavelength increases, it becomes transparent gradually. At  $\lambda > 700$  nm, the transmittance is nearly the same as that of the E7 cell. In another experiment, we compared the voltage-dependent transmittance of our SPNLC cell with the homogeneous E7 cell between crossed polarizers at  $\lambda = 1.55$   $\mu\text{m}$ . Their transmittance peaks are almost the same. This experiment proves that the SPNLC film is free from light scattering at  $\lambda = 1.55$   $\mu\text{m}$ . The transmittance result shown in Fig. 6 is consistent with our estimated domain size, which is ~500 nm, based on the response time data.

To make the SPNLC cell suitable for active matrix direct-view or color sequential displays, we need to eliminate light scattering in the entire visible spectral region and reduce the operating voltage to ~5  $V_{\text{rms}}$ . To eliminate light scattering at  $\lambda \sim 400$  nm, we could use a low birefringence LC mixture or slightly increase the monomer concentration in order to reduce domain sizes. Increasing monomer concentration would increase the operating voltage. Thus, using a low birefringence LC mixture is more feasible. However, the detailed two-step UV curing processes remain to be optimized. To reduce operating voltage, we could use a thinner cell gap or use a LC mixture with a lower threshold voltage.

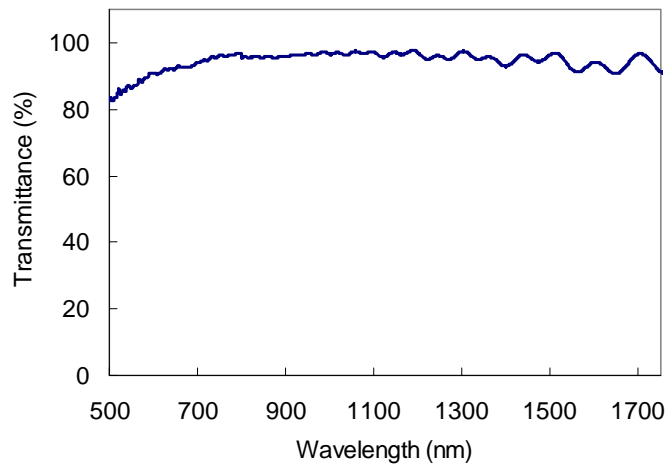


Fig. 6. Wavelength-dependent transmittance of the E7 SPNLC cell.  $d \sim 9 \mu\text{m}$ .

For fiber-optic applications, it is highly desirable that a VOA has a broad bandwidth over the whole spectral range defined by the International Telecommunication Union (ITU). To investigate the wavelength dependency, an ANDO ASE light source ( $\lambda=1525\text{-}1575 \text{ nm}$ ) and an optical spectrum analyzer were used. Figure 7 shows the wavelength-dependent attenuations of the SPNLC VOA. The attenuation variations from wavelength 1530 to 1570 nm was measured at 0, 5, 10, 15, 20, 25 and 30 dB, respectively. Based on the results, the attenuation of our VOA is rather insensitive to wavelength over the ITU C-band. In addition, the polarization-dependent-loss (PDL) stays at around  $-0.2 \text{ dB}$  over this spectral range. The insertion loss of the SPNLC cell is around  $-2\text{dB}$  due to the quadruple passes of the uncoated glass substrates. To reduce this insertion loss, anti-reflection coating of the LC cell should be considered. Moreover, in order to avoid the circulator loss, a dual fiber collimator can be employed as well.

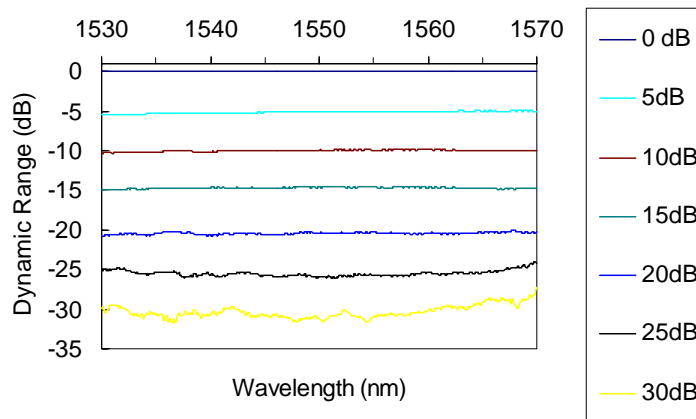


Fig. 7. The wavelength-dependent attenuations of the VOA at different attenuation range.

#### **4. Discussion**

The device depicted in Fig. 3 is in a normally-on mode. However, a normally-off VOA is also needed in dynamic optical networks for some special demands such as channel blocking and system protection. To achieve a normally-off mode, we could remove the QWP shown in Fig. 3. Since the SPNLC cell has a phase retardation  $\delta=\pi/2$  at  $\lambda=1.55 \mu\text{m}$ , the total phase retardation of the output beams is  $\pi$  after passing the modulator module twice. Therefore, the polarization states of the two retro-beams from LC cell remain linearly polarized but their axes are rotated by  $90^\circ$ . The return paths of these beams in the PBD are deviated from those of the incident beams and no light is coupled into the collimator. The VOA is normally-off at  $V=0$ . As the applied voltage increases, the transmittance increases.

#### **5. Conclusion**

In conclusion, we have demonstrated a reflective-mode VOA with  $\sim 0.24$  ms response time at room temperature ( $\sim 21^\circ\text{C}$ ) and -32 dB dynamic range using a sheared polymer-network liquid crystal. Such a VOA exhibits no light scattering at  $\lambda=1.55 \mu\text{m}$ . Its application for high speed optical networks is foreseeable.

#### **Acknowledgments**

The authors are indebted to AFOSR for financial support under contract No. F49620-01-1-0377.